UDC 621 . 746 . 047 : 620 . 192 . 49

Technical Report

Development of Steel Surface Melting Technology for Improvement of Hot Shortness Caused by Tramp Elements

Ken-ichi YAMAMOTO* Takehiko TOH
Hideki HAMATANI Keiji TSUNENARI
Kenji UMETSU Yasuo MARUKI
Sunao TAKEUCHI Yoshihiro YAMADA

Abstract

Tramp elements such as Cu cause a severe hot shortness. However, Cu is the useful alloying element for increasing hardness and improvement of the steel properties and Cu is often added to the steels. Therefore, by means of a steel surface melting technology, hot shortness should be suppressed by the addition of Ni only in the surface layer. After hot-rolled, the sheets are sandblasted and checked for surface defects due to hot shortness. There are no defects and steel samples alloyed in the surface layer are very clean. Consequently, steel containing Cu alloyed Ni in the surface layer does not indicate hot shortness at the surface.

1. Introduction

From the standpoint of energy conservation and the effective utilization of resources, it is particularly important to maximize the use of iron scrap as one of the principal raw materials in the steelmaking process. However, when tramp elements, such as copper (Cu), tin (Sn), etc., contained within iron scrap, mix with the molten steel, they cause serious problems since they can hardly be removed by the steel refining process and tend to be imparted to the final product. In a hot oxidizing atmosphere, Cu precipitates onto the steel surface in the form of a liquid and invades the austenite grain boundaries, promoting hot shortness.[1-3] Concerning the mechanism of Cu invasion into austenite grain boundaries and the propagation of cracks in carbon steel, the range of the brittleness temperature and the influences of Cu, Sn, nickel (Ni), silicon (Si), and phosphorous (P) concentrations thereon have been clarified by in-depth studies.[4-6]

On the other hand, Cu helps increase the r-value of deep drawing steel. From studies on recrystallization microstructures of low carbon steels having 0.01 ~ 1mass% Cu and a very low sol. aluminum (Al) concentration,[7-10] it is known that C (Fe_3C) in steel promotes the precipitation of Cu, or regulates the site of Cu precipitation, and that the {111} <110> recrystallization texture grows most conspicuously when approximately 0.05mass% C coexists with the Cu. In addition, it has been found possible to manufacture a high-strength, Cu-added steel having a large r-value using, as its base, so-called interstitial free steel (IF steel) which is an extra-low carbon steel added with carbide/nitride forming elements, such as titanium (Ti) and niobium (Nb).[11, 12]

Therefore, if the generation of liquid Cu, or the intergranular precipitation of Cu, in the high-temperature region of the steelmaking and hot rolling processes can be prevented,[13, 14] it becomes possible not only to ease the regulations on tramp elements contained in raw materials for steel but also to develop new high-strength steels utilizing Cu positively.

In order to neutralize the harmful effects of tramp elements, we developed a new technology whereby the surface layer of the slab, at the back of the continuous caster, is uniformly melted by means of a plasma or electromagnetic heating, and Ni, in the form of a wire, is added to the melted surface layer to prevent the Cu in the surface layer from promoting hot shortness.

2. Building a Model for Predicting Cu Content of Iron Scrap by the Year 2030

In order to evaluate the actual conditions of scrap iron as a base for the present development of technology, a model was built for predicting the amount of scrap iron expected to be generated in the future and its expected Cu content. First, the amount of scrap iron generated was estimated for each of 11 sectors—housing, non-hous-

* Senior Researcher, Steelmaking R&D Div., Process Technology Center
20-1 Shintomi, Futtsu, Chiba 293-8511

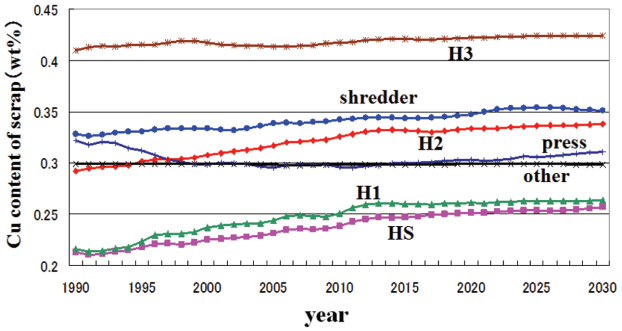

Fig. 1 Trend of the Cu content of scrap until 2030

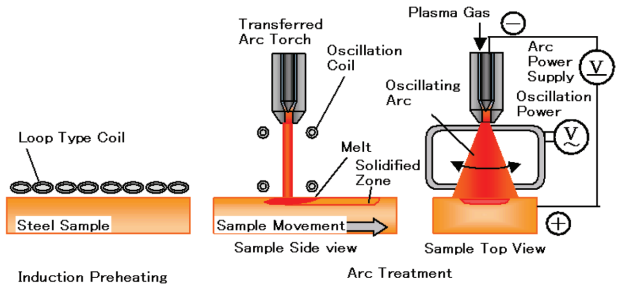

Fig. 2 Schematic illustration of experimental apparatus and sequential procedure in hot simulator [15]

Table 1 Experimental condition of hot simulator [16, 17]

Cathode material	W - 2%La_2O_3
Cathode diameter	6.4 mm
Cathode tip angle	60 degree
Cathode nozzle diameter	5 - 8 mm
Atmosphere	1 atm argon
Sample	IF steel (0.2 m × 0.125 m × 0.025 m)
Plasma gas	Ar - 2%H_2 (10 - 60 Nl/min)
Plasma current	100 - 400 A
Arc length	0.1 m
Oscillation coil current	200 A

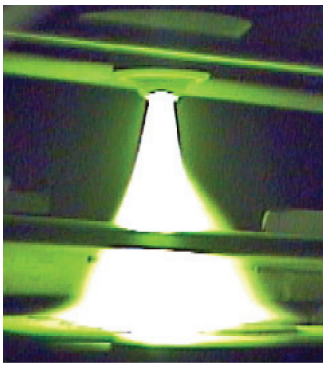

Fig. 3 Typical snapshot of DC plasma under sinusoidal AC magnetic field [16, 17]

ing, civil engineering, automobiles, shipbuilding, industrial machinery, electrical machinery, household/office equipment, containers, secondary products, and other. For the process of estimation, the stock method was applied to automobiles, housing, and non-housing, whereas the durable period method was applied to the other eight sectors. In this way, the annual amount of scrap iron generated until the year 2030 was estimated. The amount of scrap iron in 2030 was predicted to be 33,720,000 tons, which is 3,700,000 tons more than that generated in 2003.

Next, the amounts of scrap iron were evaluated by sector, by steelmaking process, and by steel grade with respect to the appropriate distribution items, a matrix of sector and final steel product for each of the distribution items was prepared, and then each distribution item in the matrix was multiplied by the appropriate Cu content specified in the JIS for final steel products. By so doing, the amount of Cu expected to derive from each distribution item was estimated. Finally, the total amount of Cu from all distribution items was divided by the total amount of scrap iron to obtain the total amount of Cu in distributed scrap iron. **Fig. 1** shows the results of the prediction of Cu content of scraps on the assumption that the Cu entrainment rate would remain unchanged from the base year of 2003. It can be seen that the Cu content of heavy scraps will increase markedly. Heavy scraps are divided into five classes—HS, H1, H2, H3, and H4—according to size and thickness. Since H2 accounts for the largest proportion, it determines the base price of iron scrap. Even in the HS/H1 high-grade scraps for which a Cu entrainment rate is not set, the content of Cu coming from steel is more than 0.25%. From Fig. 1, it can also be seen that the Cu content of H2 will increase significantly.

3. Steel Surface Melting Technology Using DC Arc Plasma

3.1 Experimental results using a hot simulator

Because of its high energy density, excellent thermal efficiency, and good stability, DC arc plasma is used as a means of heating, melting, and welding. Using the hot simulator shown in **Fig. 2**,[15] we carried out a basic experiment on the melting of a sample slab surface. The experimental conditions are shown in **Table 1**.[16, 17] After the sample slab was preheated by electromagnetic induction in an argon (Ar) atmosphere, the surface of the slab was melted by a DC arc plasma that was kept oscillating in an AC magnetic field while the slab was moving. Since a coil is installed around the DC plasma arc to apply an AC magnetic field perpendicularly to the arc, the plasma arc oscillates in the AC magnetic field and becomes fan-shaped (**Fig. 3** [16, 17]). The energy density of the arc column emitted from the tip of the torch nozzle is increased by a plasma jet condensed by the Lorentz force of the arc column itself. At the same time, the arc column is widened like a fan by an AC magnetic field applied perpendicularly to it. As a result, a high energy density can be obtained efficiently over a wide range.[18]

The sample slab was moved in the direction perpendicular to the direction of oscillation of the fan-shaped plasma arc to melt the slab surface. The appearance of the melted slab surface is shown in **Fig. 4**.[15] The slab surface is very smooth thanks to stable melting from top to bottom. In addition, the slab surface layer was improved in cleanliness because nonmetallic inclusions were removed by floatation during the melting process. **Fig. 5** shows the grain size distribution of inclusions before and after melting of the slab surface.[19] Inclusions of any size were observed to decrease in number, while the number of inclusions exceeding 20 μm were nonexistent.

3.2 Analysis of steel surface melting technology using a total model

The total model consists of three separate elements, each modeling (1) electromagnetic induction, (2) plasma, and (3) molten pool

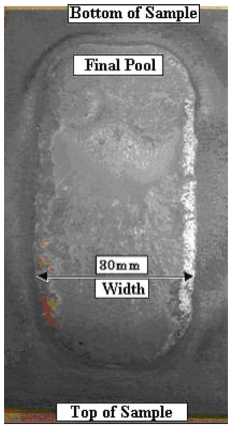

Fig. 4 Photograph of the surface of a treated sample [15]

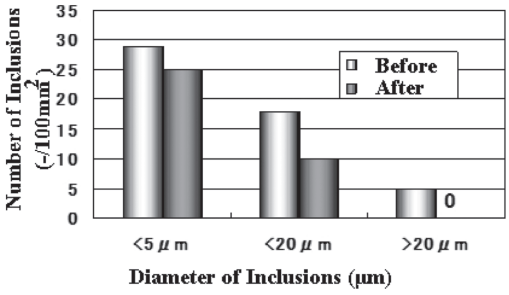

Fig. 5 Change in inclusion number [19]

flow in accordance with the following schema

(1) Electromagnetic induction
 (i) The Joule heat per unit volume at a specific location within the slab
 (ii) The Lorentz force acting upon the molten iron

(2) Plasma
 (i) Plasma heat transfer (including radiant heat) to slab surface
 (ii) The gas drag by the oscillating plasma

(3) Molten pool flow
 (i) The flow induced within the molten pool by electromagnetic induction and plasma (which includes heat convection, Marangoni convection, and electromagnetically-induced flow)
 (ii) The advective diffusion of the solute by flow of the molten pool

The numerical distributions obtained by the individual element models are then used as the boundary conditions and converted physical values for the total model. **Fig. 6** shows the relationship between the total model and the element models.[15, 20] By using a total model for the hot simulator, it is possible to reproduce the experimental results. The larger the arc current, the larger becomes the melting width. From the model, it can be concluded that this is owing to an increase in input heat per unit time/volume.

3.3 Parallel-set plasma apparatus

The parallel-set plasma apparatus (**Fig. 7**) consists mainly of: (1) 5 sets of DC plasma power supplies, torches, and lifts, (2) an atmosphere sealer/chamber, (3) a sample driver, (4) a device for preheating the sample by electromagnetic induction heating, and (5) a controller. The apparatus is capable of processing cold slabs up to 400 mm in width and 1,000 mm in length.

Using the described parallel-set plasma apparatus, we carried out

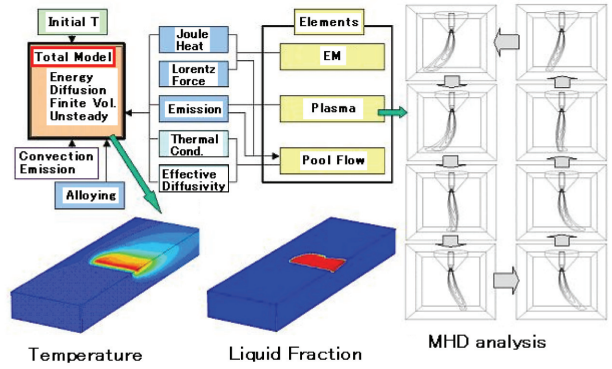

Fig. 6 Schematic illustration of the total model [15, 20]

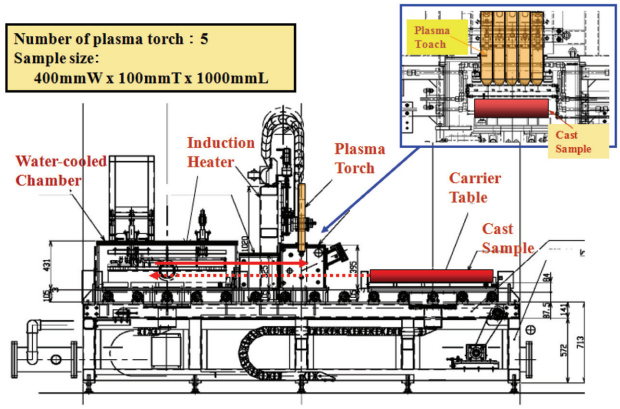

Fig. 7 Schematic illustration of the parallel-set plasma apparatus [19]

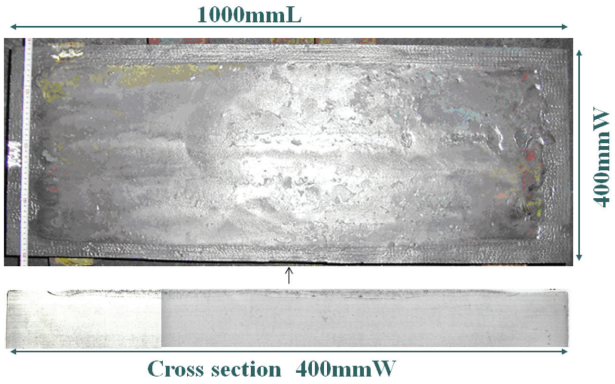

Fig. 8 Photographs of treated sample by parallel-set plasma [21]

an experiment on melting and modifying the surface layer of a slab 1 m in length and 0.4 m in width in an Ar gas atmosphere. **Fig. 8** [21] shows the appearance of the processed slab surface and the etched cross section of the slab, taken from near the center. Processed from left to right, the slab surface was uniformly melted almost entirely. From photographs of cross sections of the slab, it was confirmed that the slab surface was evenly melted to a depth of about 4 mm.

3.4 Alloying technology

In order to neutralize the harmful effects of tramp elements, we developed a new technology whereby the surface layer of the slab at the back of the continuous caster is uniformly melted by means of the apparatus described in the previous section and a prescribed

amount of Ni is added, in the form of a wire, to the melted surface layer to prevent the Cu in the surface layer from promoting hot shortness.

Fig. 9 [22] schematically shows the wire feeding system used for implementation of the proposed alloying technology. **Fig. 10** shows the effect of the wire feeding rate on the variance in the Ni content of the melted surface layer as well as on the falling frequency of molten wire droplets. It is observed that the balance between the radiant heat from the plasma/slab and the Ni melting rate improves with an increasing wire feeding rate, and, as a result, the Ni content becomes more uniform, since Ni can be fed continuously to the melted surface layer. **Fig. 11** shows the distribution of the Ni concentration under optimum alloying conditions. The results of a Ni isoconcentration analysis by an electron probe microanalyzer (EPMA) indicate that the Ni concentration is uniform both in the direction of depth and in the direction of processing width. In addition to controlling the Ni concentration of the melted surface layer by altering the wire feeding rate, it can also be controlled by adjusting the Ni content of the wire fed to the slab surface.

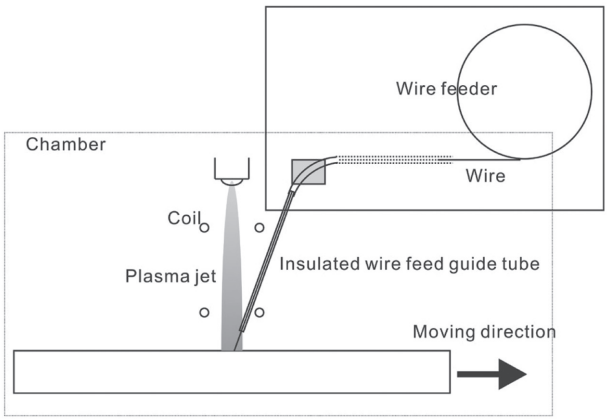

Fig. 9 Schematic illustration of wire addition experimental apparatus [22]

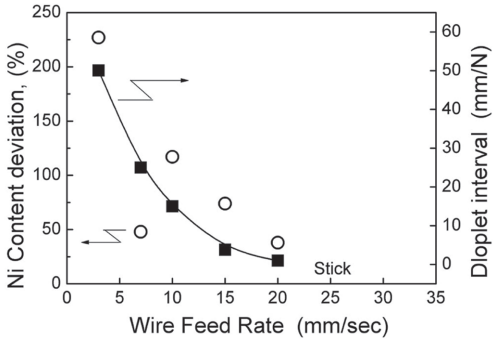

Fig. 10 Effect of wire feed rate on the frequency of molten wire droplet and Ni content deviation [22]

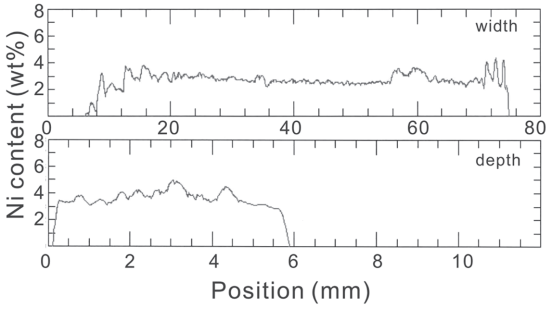

Fig. 11 Ni content distribution under optimum conditions [22]

3.5 Bench-scale test equipment

Employing the component technologies that have been previously discussed herein, we fabricated bench-scale test equipment that permits melting the surface layer of an actual slab sample (with dimensions of about 400 mm in width by 7,000 mm in length and with a thickness of 100 mm) to a depth of about 4 mm uniformly and stably and permits the addition of an alloying element to the melted surface layer. As a result of this processing, the harmful effects of tramp elements in the solidification process and slab treatment process were neutralized.

First, a 0.5%Cu IF steel slab, 400 mm wide by 7,000 mm in length and a thickness of 100 mm, was preheated and the surface layer of the slab melted using the plasma torch apparatus described in Section 3.3. A Ni wire was then fed to the melted surface layer in the manner described in Section 3.4. **Fig. 12** [23] shows an image, obtained by a high-speed video camera, of the surface layer being melted by the plasma torch apparatus. From the tips of the five plasma torches laid out in parallel, the jets are observed to reach the slab surface oscillating in synchronization with one another. The surface properties of the processed slab were good. The molten pools formed by the five plasma torches were beautifully united to provide a uniform, continuously melted surface along the length and across the width of the slab. The depth of the melted surface layer was about 4 mm. **Fig. 13** shows the Ni concentration distribution in the slab surface layer. The average Ni concentration was determined to be 1.4%, but it can be adjusted by reducing the Ni content of the wire fed to the slab surface.

After the test, the slab was first heated to 1,100°C in a reheating furnace and held at that temperature for one hour, and then subjected to hot rolling. With a finishing temperature of 900°C, a hot-rolled plate 4 mm in thickness was obtained. No cracks were observed to occur in the slab during the reheating and hot-rolling processes. Both the processed and non-processed surfaces of the hot-rolled plate were subjected to sand blasting and color checking in order to inspect for cracks, defects, etc. Although the non-processed surface had several defects, the processed surface was completely free of cracks. Therefore, it is confirmed that the slab surface alloying technology discussed has a demonstrable effect upon the occurrence of hot shortness caused by Cu.

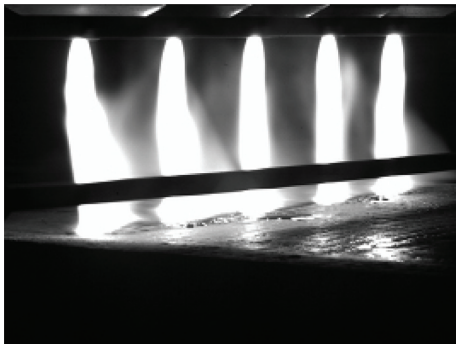

Fig. 12 Typical snapshot of DC plasma under sinusoidal AC magnetic field [23]

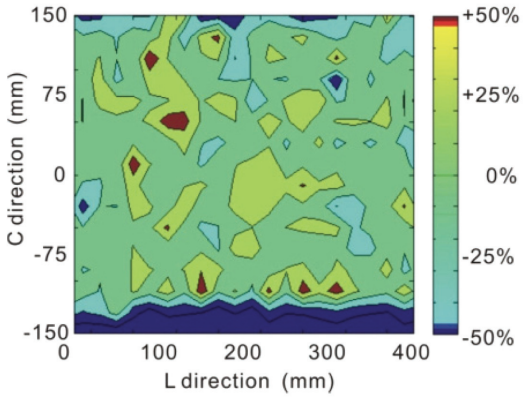

Fig. 13 Ni content of the surface of a treated sample [23)]

4. Conclusion

In order to neutralize the harmful effects of tramp elements, we developed a new technology whereby the surface layer of the slab at the back of the continuous caster is uniformly melted by means of plasma or electromagnetic heating and Ni, in the form of a wire, is added as an alloying agent to the melted surface layer to prevent Cu in the surface layer from promoting hot shortness of the slab. Following an experiment with a hot simulator, the development of a total model, an experiment with a parallel-set plasma apparatus, and an experiment with a parallel-set plasma apparatus, we fabricated bench-scale test equipment that permitted melting the surface layer of a slab sample, 400 mm wide by 7,000 mm in length and a thickness of 100 mm, to a depth of about 4 mm uniformly and stably, and allowed for the addition of an alloying element to the melted surface layer to neutralize the harmful effects of the tramp elements. By adding Ni to the surface layer of hot-rolled plate of the processed slab, hot shortness of the surface caused by Cu was restrained.

Acknowledgments

The present study is a part of the national project "Development of Technologies, etc. Relating to Materials for Social Infrastructure for Rational Use of Energies" that was carried out by the Nippon Steel Corporation with a subsidy by the Ministry of Economy, Trade and Industry.

References

1) Born, K.: Stahl Eisen. 73, 1268 (1953)
2) Melford, D.A.: J. Iron and Steel Inst. 200, 290 (1962)
3) Nicholson, A. et al.: J. Iron and Steel Inst. 203, 1007 (1965)
4) Kajitani, T. et al.: Tetsu-to-Hagané. 81, 185 (1995)
5) Imai, N. et al.: ISIJ Int. 37, 217 (1997)
6) Seo, S. et al.: ISIJ Int. 37, 240 (1997)
7) Rickett, R.L. et al.: Trans. Am. Soc. Met. 51, 310 (1959)
8) Abe, H. et al.: Tetsu-to-Hagané. 60, 1496 (1974)
9) Abe, H.: Recrystallization and Crystalline Texture of Steel Sheet. Edited by the Recrystallization Sectional Meeting of Joint Research Committee on Fundamentals of Iron and Steel, 1974, p. 135
10) Era, H. et al.: Tetsu-to-Hagané. 70, 1946 (1984)
11) Kishida, K. et al.: Tetsu-to-Hagané. 76, 759 (1990)
12) Morita, M. et al.: Tetsu-to-Hagané. 80, 48 (1994)
13) Hasegawa, H. et al.: ISIJ Int. 43, 1021 (2003)
14) Yamamoto, K. et al.: Tetsu-to-Hagané. 90, 781 (2004)
15) Takeuchi, S. et al.: High Temp. Mat. Proc. 10, 525 (2006)
16) Yamamoto, K. et al.: The 5th International Symposium on Electromagnetic Processing of Materials. 2006, Sendai, Japan, ISIJ, p. 714
17) Yamamoto, K. et al.: CAMP-ISIJ. 20, 818 (2007)
18) Takeda, K.: Kouon Gakkai-shi. 16, 357 (1990)
19) Toh, T. et al.: The 6th International Symposium on Electromagnetic Processing of Materials. 2009, Dresden, Germany, ISIJ, p. 223
20) Toh, T. et al.: ISIJ Int. 45, 947 (2005)
21) Yamamoto, K. et al.: CAMP-ISIJ. 21, 1206 (2008)
22) Hamatani, H. et al.: Preprint for Sept. 2007 Autumn Meeting of the Japan Welding Society
23) Yamamoto, K. et al.: CAMP-ISIJ. 20, 905 (2009)

Ken-ichi YAMAMOTO
Senior Researcher
Steelmaking R&D Div.
Process Technology Center
20-1 Shintomi, Futtsu, Chiba 293-8511

Takehiko TOH
Chief Researcher, Dr.
Mathematical Science & Technology Research Lab.
Advanced Technology Research Laboratories

Hideki HAMATANI
Chief Researcher, Dr.Eng.
Nagoya R&D Lab.

Keiji TSUNENARI
Manager
Plant Engineering Div.
Plant Engineering and Facility Management Center

Kenji UMETSU
Manager
Systems & Control Engineering Div.
Plant Engineering and Facility Management Center

Yasuo MARUKI
Department Manager
Plant Engineering Div.
Plant Engineering and Facility Management Center

Sunao TAKEUCHI
Senior Researcher
Mathematical Science & Technology Research Lab.
Advanced Technology Research Laboratories

Yoshihiro YAMADA
Senior Researcher, Dr.Eng.
Mechanical Engineering Div.
Plant Engineering and Facility Management Center